Available online at www.sciencedirect.com
SCIENCE DIRECT®
Geochimica et Cosmochimica Acta 70 (2006) 1928–1938
Geochimica
www.elsevier.com/locate/gca

Arsenous acid ionisation in aqueous solutions from 25 to 300 °C

V.P. Zakaznova-Herzog [1], T.M. Seward *, O.M. Suleimenov

Institute for Mineralogy and Petrology, ETH Zürich, Swiss Federal Institute of Technology, Zürich, Switzerland

Received 23 November 2004; accepted in revised form 12 January 2006

Abstract

The ultraviolet spectra of dilute, aqueous arsenic (III)-containing solutions have been measured from 25 to 300 °C at the saturated vapour pressure. From these measurements, the equilibrium constant was obtained for the reaction

$$H_3AsO_3 \rightleftarrows H^+ + H_{2As}O_3^-;$$

for which pK_1 (arsenous acid) decreases from 9.25 to 7.11 over a temperature range from 25 to 300 °C. In addition, electrospray mass spectrometric measurements support the conclusion that the arsenous acid moeities in low density aqueous media are $HAsO_2$ and AsO_2^-.

1. Introduction

Arsenic is widely distributed throughout the Earth crust as well as the biosphere and is involved in many geochemical and biochemical processes. It occurs ubiquitously in migrating hydrothermal fluids and precipitates in ore depositing environments as sulphides, arsenides, and sulphosalts but the transport and deposition chemistry is not well known (Heinrich and Eadington, 1986). The association of arsenic with gold in many hydrothermal systems is well documented but is also poorly understood. High concentrations of arsenic also occur in the surface precipitates of many active geothermal systems such as in New Zealand, Kamchatka, Japan, and Central and South America and elsewhere (Weissberg et al., 1979; Krupp and Seward, 1987; Smith et al., 1987; Criaud and Fouillac, 1989; Webster and Nordstrom, 2003; Reyes et al., 2003). Arsenic concentrations of geothermal fluids (i.e., from wells) are generally in the range from 0.1 to 50 mg/kg (Ellis and Mahon, 1977; Krupp and Seward, 1987; Yokoyama et al., 1993; Romero et al., 2003; Webster and Nordstrom, 2003; Polya et al., 2003) with the highest values being reported for the El Tatio system in Chile.

There is also considerable interest in ambient temperature aqueous arsenic geochemistry (i.e., Ryu et al., 2002; Smedley and Kinniburgh, 2002; Chaillou et al., 2003; Polya et al., 2003) because of the important environmental implications. In addition, any understanding of the biochemical role of arsenic in the microbial world (Newman et al., 1997; Salmassi et al., 2002) is premised on a knowledge of the arsenic speciation in the relevant environment (Nickson et al., 2000; Caldwell et al., 2003).

In order to evaluate and model the aqueous arsenic chemistry in natural systems over a wide range of conditions from ambient to hydrothermal, reliable thermodynamic data are required for arsenous acid. With the exception of the high and apparently spurious value for the ionisation constant reported by Garrett et al. (1940) (i.e., $pK_1 = 9.62$), the ambient temperature values of pK_1 are in the range of $9.2 \leqslant pK_1 \leqslant 9.3$. Antikainen and Tevanen (1961) and Yamazaki et al. (1993) have also measured pK_1 values up to 45 and 65 °C respectively and a few experimentally determined values have been reported at higher

* Corresponding author. Fax: +41 (0)1 632 10 88.
E-mail addresses: herzog@erdw.ethz.ch (V.P. Zakaznova-Herzog), tseward@erdw.ethz.ch (T.M. Seward).
[1] Present address: Institute of Isotope Geochemistry and Mineral Resources, ETH Zürich, Swiss Federal Institute of Technology, Zürich, Switzerland.

0016-7037/$ - see front matter © 2006 Elsevier Inc. All rights reserved.
doi:10.1016/j.gca.2006.01.014

temperatures (e.g. Pokrovski, 1996). The available thermodynamic data for arsenous acid ionisation (K_1) for the temperature interval around 25 °C are summarised in Table 1.

In a number of papers (Antikainen and Rossi, 1959; Yamazaki et al., 1993), arsenous acid is considered to have the stoichiometry $HAsO_2$. On the another hand, there are a number of other studies in which arsenous acid is considered as a moeity comprising one arsenic atom coordinated by three OH^--ligands (Loehr and Plane, 1968; Pokrovski et al., 1996; Gout et al., 1997; Raposo et al., 2003). This interpretation is supported by Raman spectra (Loehr and Plane, 1968; Pokrovski et al., 1996; Gout et al., 1997). Loehr and Plane (1968) studied As(III)-containing solutions with OH/As ratios ranging from 3.5 to 15 and interpreted the observed Raman lines in terms of four distinct chemical species, which were assigned to $As(OH)_3^0$, $AsO(OH)_2^-$, $AsO_2(OH)^{2-}$ and AsO_3^{3-}. Our own rank analysis of their data indicates the presence of only two or three different species. The recent studies by Gout et al. (1997) and Pokrovski et al. (1996) (i.e., Raman measurements from 20 to 275 °C and solubility measurements at 250 and 300 °C) have been interpreted in similar way to those of Loehr and Plane (1968) and are thus consistent with their original conclusions and band assignments. It should also to be noted that the solutions studied in the above mentioned studies were for the most part quite concentrated. Pokrovski et al. (1996) and Gout et al. (1997) studied solutions having arsenic concentrations in the range 0.02–5.2 m. Loehr and Plane (1968) report the As concentrations of their solutions by stating only that OH + As(III) was always >8 mol/dm^3 and for which it may be inferred that their arsenic concentrations were 0.2–1.8 mol/dm^3. Their data do not necessarily represent arsenic(III) hydrolysis behavior in more dilute solutions in which As $\leqslant$ 0.0001 m. As noted by Gout et al. (1997) and Tossell (1997), the Raman spectra of concentrated aqueous arsenic solutions exhibit clear evidence for the presence of polymeric species such as $As_3O_3(OH)_3$.

Exafs data may also provide information on the As(III)-oxygen coordination environment. Pokrovski et al. (2002) obtained Exafs data on the As–OH system (As $\simeq$ 0.3 m) and concluded that each As atom is surrounded by three oxygens at a distance of 1.78 Å. The conclusion that arsenous acid exists as $As(OH)_3$ is not necessary conclusive. The Exafs data provide information about average number of surrounding oxygens and the possibility exists that As^{3+} is coordinated to three, non-equivalent oxygens, that is, two oxygens, one of which is protonated together with a solvated water molecule.

A recent study of Debusschere et al. (2000) of arsenic speciation using capillary zone electrophoresis coupled mass spectrometry supports the $HAsO_2$ stoichiometry. The As-containing species produced in the gas phase had mass-to-charge-ratios (m/z) of 107 and indicated the presence of the AsO_2^- ion (molecular mass of $AsO_2^- = 75 + 2.16 = 107$).

This study primarily focuses on the determination of the arsenous acid ionisation constant from 25 to 300 °C by means of high temperature, flow-through UV spectrophotometry. We have also carried out fundamental ab initio calculations as well as electrospray mass spectrometric measurements on arsenic-containing solutions in order to gain additional insight into arsenous acid stoichiometry.

2. Experimental methods

Mass spectrometric measurements for this study were carried out using the electrospray ionization (ESI) technique with a Surveyor MSQ (Thermo Finnigan) mass spectrometer. In order to obtain a mass spectrum from an As(III)-containing solution, the sample is passed along a narrow metal capillary tube, the end of which is maintained at a high potential of around 2.5 kV. The high potential and small radius of curvature at the end of the capillary tube creates a strong electric field which causes the emerging liquid to leave the end of the capillary as a mist of droplets mixed with vapour (i.e., nebulization) and occurs at near atmospheric pressure. Solutions for mass spectrometric analysis were prepared by dissolving As_2O_3 in perchloric acid or sodium hydroxide solutions and were in the pH range from 6 to 10.

All solution preparation and handling as well as the titration of solutions were carried out in such a way as to exclude any contact with air and under argon in order to

Table 1
Previously reported values for the ionisation constant of arsenous acid at ambient temperature; I is the ionic strength

T (°C)	pK_1	I	Method	References
18	9.21–9.28	0–0.875	Potentiometry	Britton and Jackson (1934)
25	9.62	0–0.3	Solubility/pH meas.	Garrett et al. (1940)
25	9.294	0	Potentiometry	Antikainen and Rossi (1959)
25	9.28	0	Potentiometry	Salomaa et al. (1969)
25	9.178	0.05	Potentiometry	Antikainen and Tevanen (1961)
22	9.32 ± 0.01	0.5	Spectrophotometry	Ivakin et al. (1976)
	9.21 ± 0.01	1		
25	9.45	0.1	Ion ex./polarogr.	Nishida and Kimura (1989)
25	9.32 ± 0.05	0	Potentiometry	Pokrovski (1996)
25	9.243 ± 0.003	0	Spectrophotometry	Yamazaki et al. (1993)
25	9.22 ± 0.01	0	Potentiometry	Raposo et al. (2003)

avoid oxidation of As(III) to As(V) and CO_2 contamination. An arsenic(III) stock solution (0.1877 m) was prepared by dissolving a weighed amount of As_2O_3 in NaOH solution. Experimental solutions were prepared by addition (excluding air and employing gas tight Hamilton syringes) of a weighed amount of the stock solution and standardised sodium hydroxide solution to degassed water. The total arsenic concentrations in these samples were determined by ion-chromatography as well as by flame atomic absorption spectroscopy and gravimetric analysis. Precise Na^+ concentrations of the arsenic-containing and NaOH blank (no arsenic) solutions were obtained by titration with potassium hydrogen phthalate (KHP). Titrations were performed under argon with a Metrohm 736 GP Titrino autotitrator driven by TiNet 2.3 software.

The ultraviolet spectra were collected using a high temperature, flow-through titanium/palladium alloy cell which was placed in a Cary 5E double beam spectrophotometer. The optical cell had UV quality quartz glass windows and a thermocouple controlled cooling/heating system to ±0.5 °C. The flow-through system enables the solution composition to be changed without opening the system or disturbing to the optical settings such as for example, the path length or the positioning of the cell in the light path. In order to maintain single phase conditions, the pressure was held at 15 bar above the saturated water vapour pressure and controlled by means of a Dynamax SD-300 HPLC pump and an adjustable back pressure regulator. The overall experimental setup is shown schematically in Fig. 1. The UV spectra of As(III) species were recorded from 190 to 300 nm at seven temperatures from 25 to 300 °C. Fig. 2 shows measured spectra of arsenous acid species at 25 and 300 °C. The concentration range of the total dissolved arsenic(III) in the experimental solutions was varied from 9.01×10^{-5} to 1.8×10^{-3} mol/dm^3 and the pH from 4.00 to 10.96 by addition of perchloric acid or sodium hydroxide. Fig. 3 shows the spectra of NaOH solutions (blanks) at 25 °C. Table 2 gives the solution compositions pertaining to the measured spectra. All spectra at all temperatures were corrected for water solvent and silica window background absorbance. To relate the molar concentration scale of the Beer–Lambert law to the molal scale of standard thermodynamic convention, the measured absorbances, A^{obs}, were corrected for

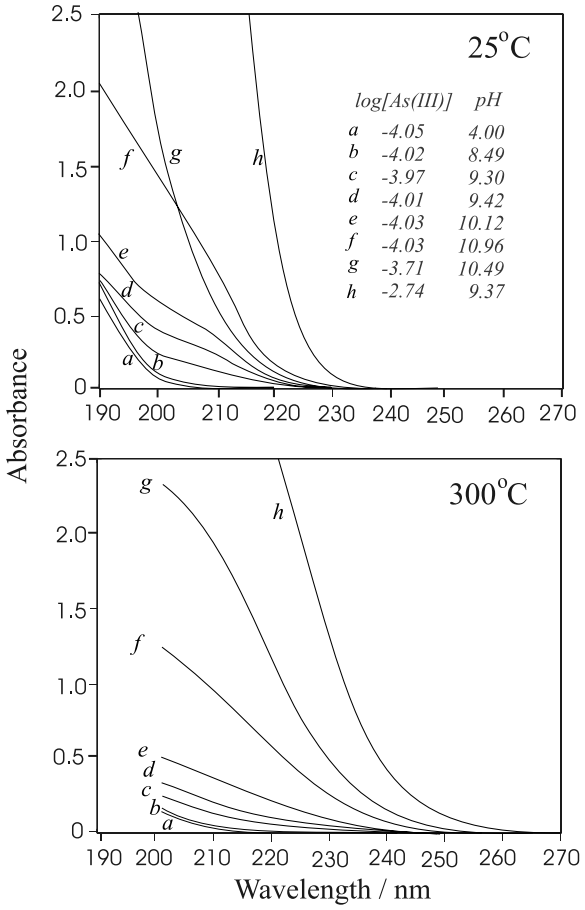

Fig. 2. Spectra of arsenic (III)-containing solutions, corrected for water and silica window background absorbance at 25 and 300 °C at the saturated water vapour pressure.

the isothermal variation of solution density at each temperature. The experimental solutions were dilute (i.e., <0.003 mol/dm^3) and hence the densities were taken as for pure water from Haar et al. (1984).

3. Results and discussion

3.1. Mass spectrometric measurements

The mass spectra of two solutions having an arsenic concentration of 2.3×10^{-4} mol/dm^3 (Fig. 4) are character-

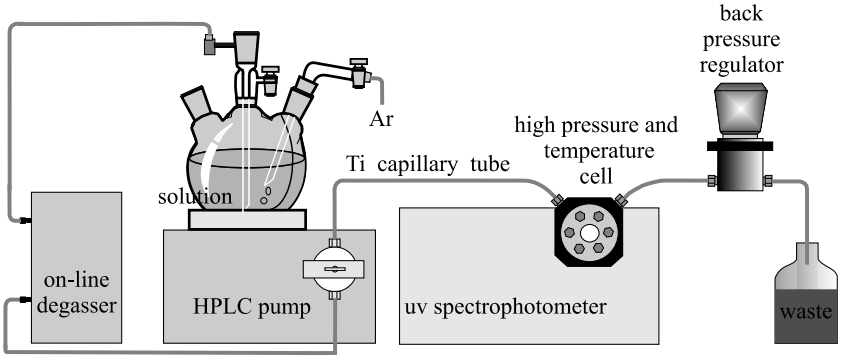

Fig. 1. Experimental setup.

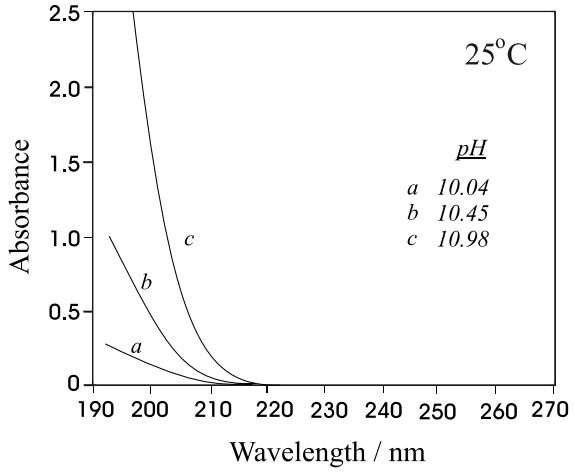

Fig. 3. Spectra of NaOH solutions, corrected for water and silica window background absorbance at 25 and 300 °C at the saturated water vapour pressure.

Table 2
Compositions of experimental solutions used for arsenous acid ionisation constant evaluation from 25 to 300 °C; concentrations in mol/dm^3

	As concentration	Na concentration
Solution		
1	0.0000958	0.0000172
2	0.0001065	0.0000765
3	0.0000925	0.0002122
4	0.0001935	0.0004908
5	0.0000932	0.0011881
6	0.0000968	0.0000840
7	0.0000967	0.0001184
8	0.0000486	0.0002823
9	0.0000939	0.0009938
10	0.0000901	—
11	0.0018296	0.0010667
Blanks		
1	—	0.00010976
2	—	0.00028649
3	—	0.00095796

ised by a number of strong peaks, one of which has $m/z = 107$ and is due to the presence of ionised monomeric arsenous acid, [O = As–O$^-$], whereas for $H_2AsO_3^-$, $m/z = 125$ and was not detected. The other peaks arise inherently from other components in the solutions as shown in Table 3. The electrospray mass spectra indicate that the AsO_2^- moeity is the dominant arsenic-containing species present, however, these data do refer, a priori, to the gaseous state and not rigorously to the solution (liquid) phase.

3.2. Ab initio calculations

In order to provide insight into the stoichiometry of arsenous acid, ab initio calculations were also undertaken. Current progress in the computation of total energies of molecules at their equilibrium geometries permits the prediction of atomisation energies to an accuracy better than

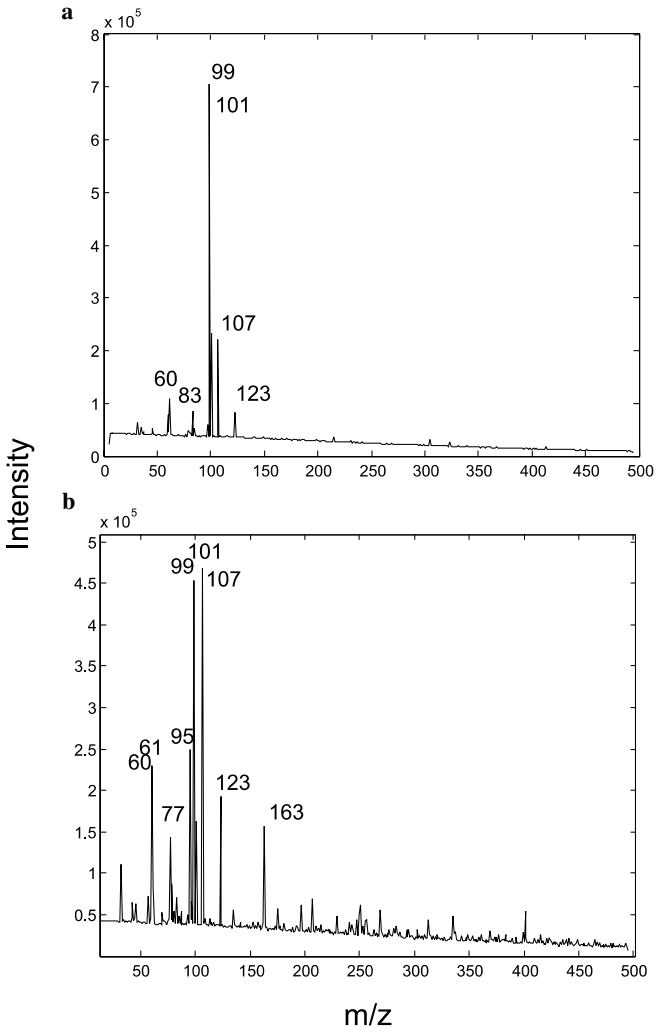

Fig. 4. Mass spectra of As_2O_3(s) dissolved in, (a) perchlorate solution and (b) As_2O_3(s) dissolved in water–sodium hydroxide solution; the arsenic concentration of both solutions is 2.3×10^{-4} mol/dm^3; m/z is mass-to-charge ratio.

Table 3
Identification of the peaks in the mass spectra (Figs. 4a and b) obtained from solutions having As = 2.3×10^{-4} mol/dm^3

m/z, in (a)	Formula	m/z, in (b)	Formula
99	$^{35}ClO_4^-$	99	$^{35}ClO_4^-$
101	$^{37}ClO_4^-$	101	$^{37}ClO_4^-$
		77	^{77}As or $^{13}CO_4$
107	AsO_2^-	107	AsO_2^-
123	$As(V)O_3^-$	123	$As(V)O_3^-$

±8 kJ/mol and comparing well with experimental data. Dielectric continuum theories are now widely used to describe hydration in conjunction with quantum mechanical calculations. We have applied the G2 model approach combined with polarisable continuum model (PCM-SCRF) calculations at the MP2/6-311+G(3df,2p) level to address solvation effects. All structures were optimised in the gas phase and all stationary points were characterised

Table 4
Calculated gas phase energies (G°_{g}) and Gibbs solvation (solution) free energies (G°_{sol}) at 298 K

	A		B	
	G°_{g}(hartree)	G°_{sol}(kJ mol^{-1})	G°_{g}(hartree)	G°_{sol}(kJ mol^{-1})
H_3AsO_3	−2461.611647	−43.39	−2463.498412	−52.97
$H_2AsO_3^-$	−2461.064497	−269.66	−2462.950264	−257.57
$HAsO_2$	−2385.234684	−12.26	−2387.014090	−28.62
AsO_2^-	−2384.695946	−271.67	−2386.471505	−255.10
OH^-	−75.729025	−470.99	−75.837863	−348.23
H_2O	−76.349651	−29.16	−76.459605	−24.10

A, energies calculated with G2/PCM model with geometries optimised in a gas phase; B, energies calculated using DFT at the B3LYP/6-311+(3df, 2p) level and with geometries optimised in solution within the PCM model.

by frequency calculations at the same level. Calculations were carried out with Gaussian98 suite of programs (Frisch et al., 2001). The UAHF cavity (the default cavity for Gaussian98) was chosen for the PCM calculations. A dielectric constant of 78.4 was used in order to simulate the aqueous environment. The standard state for the gas phase and solution thermodynamic properties was chosen as 1 mol/dm^3. The gas phase energies and hydration (solvation) free energies are given in Table 4.

The PCM calculations were carried out on the isocoulombic reactions of the type

$$HA + OH^- \rightleftarrows A^- + H_2O \quad (1)$$

in order to minimise the large computational errors which arise because of the imbalance of charged species as noted for example by Pliego and Riveros (2002) and Takano and Houk (2005). The value of pK_1 for the aqueous arsenous acid ionisation as defined by either:

$$H_3AsO_3 \rightleftarrows H^+ + H_2AsO_3^- \quad (2)$$

$$\text{or, } HAsO_2 \rightleftarrows H^+ + AsO_2^- \quad (3)$$

was then calculated in the conventional way from

$$pK_1 = \frac{\Delta G^{\circ}_{sol}}{2.3026\ RT} + 15.74, \quad (4)$$

where ΔG°_{sol} is the computed Gibbs energy of solvation derived from the individual G^{o}_{sol} values given in Table 4. The second term (i.e., 15.74) includes pK_w as well as the mole fraction to mol/dm^3 conversion factor.

The calculated pK_1 at 25 °C for reaction (2) in solution is 19.92 and for the reaction (3), is 10.01. This latter value is close to our experimentally determined value of 9.25 as well as to the other reliable literature data (Table 1). Thus, the G2/PCM model calculations apparently support the $HAsO_2$ stoichiometry. However, it should be kept in mind that the quantum mechanically calculated values of pK_1 given above refer to rigid geometries optimised in the gas phase. Thus, the geometries employed are not the relaxed configurations optimised in the PCM calculations.

In order to further consider the effect of geometry relaxation, we also performed DFT B3LYP/6-311+(3df, 2p) optimisation in the solution phase using the PCM model. The characteristic features for the geometries optimised in the solution within the polarized continuum model were slight increases in the O–H distance of ~0.02 Å as well as in the As–O distance of 0.01 Å. In addition, there was an opening of the O–As–O angle in the $As(OH)_3$ molecule by 3°. For the AsO(OH) molecule, an increase in the As = O distance and O–H distance in solution of 0.01 Å was observed, whereas the As–O distance decreased by 0.01 Å as did the O–As–O angle by 0.1°. However, the resulting values of pK_1 for reactions (2) and (3) are 2.8 and −3.6, respectively. These values are very different from the values calculated with the combined G2/PCM model in which the geometries were optimised in the gas phase only. On the basis of the quantum chemical calculations, we are thus unable to unambiguously determine which arsenous acid stoichiometry is the most stable in aqueous media. This reflects the inadequacy of the PCM model (cavity in a dielectric continuum) in describing the aqueous arsenous acid system. We further note that the gas phase calculation of Tossell (1997) which indicates a higher stability for the $As(OH)_3$ moeity is not strictly relevant to the aqueous solution environment.

The main evidence for the presence of H_3AsO_3 (i.e., $As(OH)_3$) in aqueous media comes from the Raman spectroscopic study of Loehr and Plane (1968) and a subsequent theoretical study of Tossell (1997). However, the partly qualitative nature of the band assignments as well as the applicability of the Raman spectra which pertain to concentrated media still leaves some doubt as to the stoichiometry of arsenous acid in dilute solutions. Nevertheless, the Raman data cannot be ignored and we have therefore expressed the stoichiometry of arsenous acid throughout this paper as $H_3AsO_3/H_2AsO_3^-$.

3.3. Data treatment and interpretation of UV spectra

The first part of the data treatment considers the potentiometric titrations from which pH and sodium concentrations are obtained for each arsenic-containing solution. The mathematical treatment of the potentiometric data involved the solution of six equations containing seven variables and including charge and mass balance equations as well as the expressions for the ion product constant for water and the ionisation constants of potassium hydrogen phthalate (KHP) and arsenous acid. The relevant equations are

$$K_1 = \frac{[H_2AsO_3^-]\gamma_{H_2AsO_3^-}[H^+]\gamma_{H^+}}{[H_3AsO_3^\circ]\gamma_{H_3AsO_3^\circ}}, \quad (5)$$

$$[As]_{tot} = [H_2AsO_3^-] + [H_3AsO_3^\circ], \quad (6)$$

$$K_w = [H^+]\gamma_{H^+}[OH^-]\gamma_{OH^-}, \quad (7)$$

$$K_{KHP} = \frac{[H^+][P^{2-}]}{[HP^-]}, \quad (8)$$

$$[Phtal]_{tot} = [HP^-] + [P^{2-}], \quad (9)$$

$$[K^+] + [Na^+] + [H^+] = [OH^-] + [H_2AsO_3^-] + [HP^-] + 2[P^{2-}], \quad (10)$$

where the terms in square brackets are molar concentrations (mol/dm^3); $[As]_{tot}$ is the total arsenic concentration; $[Phtal]_{tot}$ is the total potassium hydrogen phthalate concentration; K_1 is the ionisation constant for arsenous acid; K_w is the ion product constant of water and K_{KHP} is stability constant for the reaction:

$$HP^- \rightleftarrows P^{2-} + H^+. \quad (11)$$

Because the solutions were basic, the ionisation of arsenous acid has an influence on the equivalent point of the titration curve and must also be considered. The total arsenic concentration, $[As]_{tot}$, K_w, and K_{KHP} are known, as is the concentration of the standard KHP solution and the volume of KHP solution added at the equivalent point and hence, $[Phtal]_{tot}$.

The mathematical solution of the above system of equations to obtain pH and the concentrations of Na^+ was facilitated using a set of programmes developed using the MATLAB and MAPLE computational platforms. The principle of ''looking for a mathematical solution'' is based on the minimisation of the sum of squares of the differences between the experimental and theoretical titration curves (Fig. 5) as a function of Na^+ concentration, bearing in mind that the pH is given by the concentration of sodium hydroxide in the solution. The concentration of Na^+ was used in the determination of the ionisation constant for arsenous acid at higher temperatures since the direct experimental measurement of OH^- concentrations or pH in such solutions, was not possible.

The treatment of the spectrophotometric data proceeded as follows. Prior to the refinement of the equilibrium constants, it is of interest (and necessary) to validate the model in both a chemical and statistical sense. The validation is based initially on the analysis of the absorbance matrix in order to determine the number of absorbing species at each temperature. Since absorbance is a linear function of concentration for a given absorbing species at a specified wavelength, the maximum number of linearly independent columns of the absorbance matrix (i.e., the rank of the absorbance matrix) gives the number of absorbing species in solution at a particular temperature, providing that no two species have identical molar absorptivities. Once the number of absorbing species has been established, one then proceeds to the iterative calculation scheme (Fig. 6).

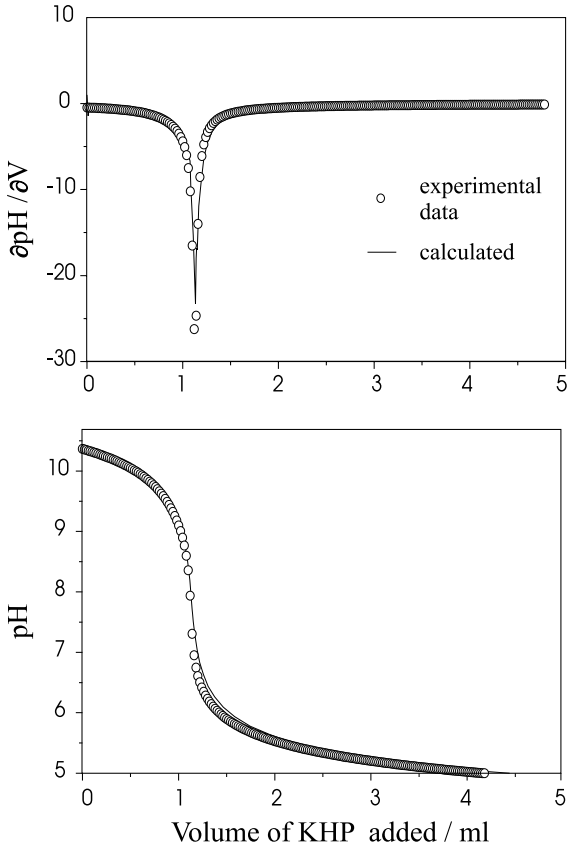

Fig. 5. Experimental and theoretical titration curves obtained for a solution having As(III) = 4.86×10^{-5} mol/dm^3 and $Na^+ = 2.82 \times 10^{-4}$ mol/dm^3(solution 8 in Table 2).

The chemical model includes the ionisation of arsenous acid

$$H_3AsO_3(aq) \rightleftarrows H^+ + H_2AsO_3^- \quad (12)$$

the ionisation of water and the ion pairing of sodium hydroxide. The computational model to obtain K_1 Eq. (5) for the reaction (12) requires consideration of the mass balance Eqs. (6 and 7), as well as the charge balance equation

$$[H^+] + [Na^+] = [OH^-] + [H_2AsO_3^-] \quad (13)$$

and the equilibrium expression for the equilibrium association constant of sodium hydroxide is

$$K_{ass} = \frac{[NaOH]\gamma_{NaOH}}{[Na^+]\gamma_{Na^+}[OH^-]\gamma_{OH^-}}, \quad (14)$$

where the terms in square brackets are molar concentrations of species in mol/dm^3; γ is the activity coefficient. Activity coefficients were calculated using an extended Debye–Hückel equation (Robinson and Stokes, 1968) although in fact, they are negligible and less than the experimental error. Furthermore, the association of sodium hydroxide becomes more significant at high temperatures (Ho et al., 2000), but at the concentrations used in this study, it affects only the second decimal place of pK_1 at 300 °C and is again less than the experimental error.

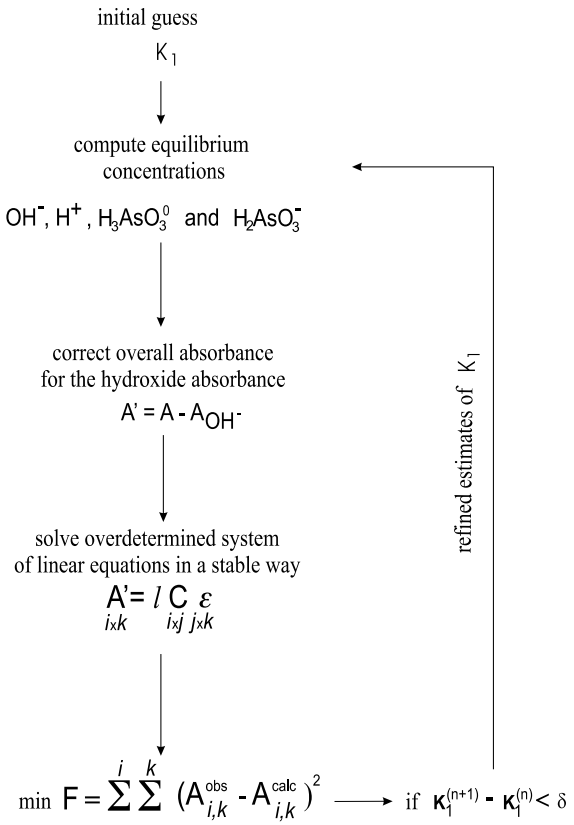

Fig. 6. Scheme of ionisation constant calculation procedure.

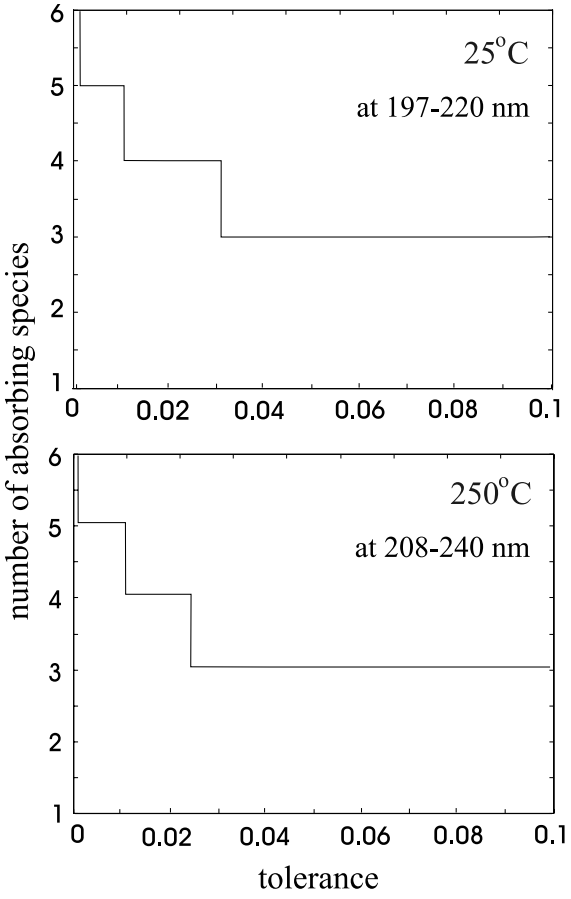

Fig. 7. Rank analysis of the absorbance matrix at 25 and 250 °C for the eight arsenic-containing solutions, the spectra of which at 25 °C are shown in Fig. 2 and the compositions for both temperatures given in Table 2.

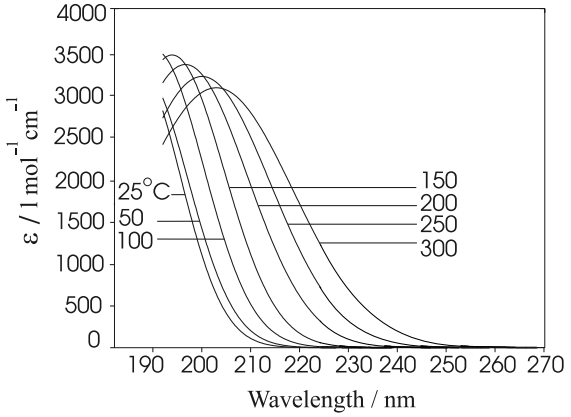

Fig. 8. The molar absorptivity, ε, of OH^- from 25 to 300 °C at saturated vapour pressures.

The aim of the iterative calculation procedure is to refine the equilibrium constant for arsenous acid, K_1. It has two features that distinguish it from conventional computation schemes. First, a correction for the contribution of OH^- absorbance to each spectrum is carried out at every iteration step. And second, the solution of the overdetermined system of linear equations is carried out in a stable way using the Tikhonov regularization technique since the system is ill-conditioned and ill-posed (Morozov, 1993).

3.4. Arsenous acid ionisation

The measured spectra represent an overlay of the contribution of all absorbing species to the absorption envelope in the range from pH 4.00 to 10.96 as shown in Fig. 2. Fig. 7 demonstrates that the rank analysis of the absorbance versus wavelength matrix created from the spectra at 25 and 250 °C for the wavelength intervals from 197 to 220 nm at 25 °C and from 208 to 240 nm at 250 °C, is three. There are thus three species in solution (i.e., the rank is three), one of which can be attributed to the hydroxide ion through its charge-transfer-to-solvent transition and associated absorption band as shown in Figs. 3 and 8. At 300 °C, the rank of the absorbance matrix for the interval 220–240 nm is 2, indicating the presence of only two absorbing species (i.e., OH^- and an arsenous acid species), whereas for the interval 240–250 nm, the rank was one, indicating the presence of only one absorbing arsenous acid species (Fig. 9). The molar absorptivities of hydroxide from 25 to 300 °C at saturated vapour pressures were obtained from UV spectroscopic measurements of the sodium hydroxide–water system and are shown on the Fig. 8. We are now left with the task of determining the identity of the two remaining species. The spectra collected from pH ≈ 4 to 8 (i.e., spectra a and b in Fig. 2) were identical,

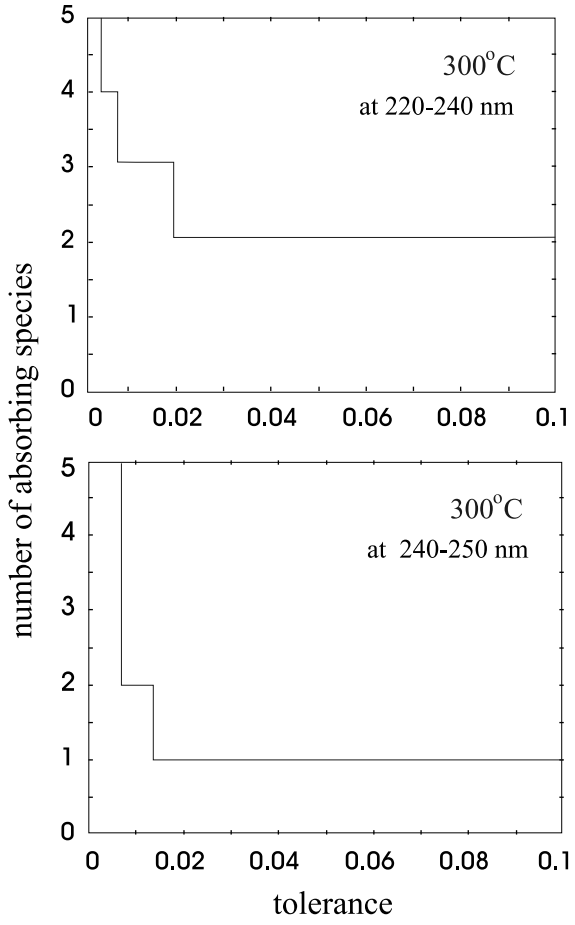

Fig. 9. Rank analysis of the absorbance matrix at 300 °C for the eight arsenic-containing solutions, of which the spectra are shown in Fig. 2 and the compositions are given in Table 2.

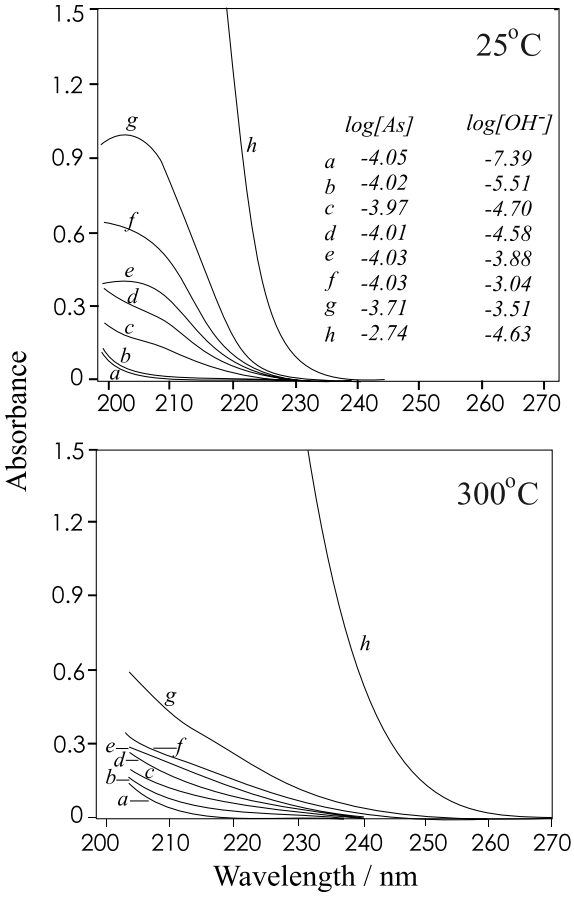

Fig. 10. Spectra of As(III)-containing solutions corrected for water and silica window background absorbance as well as for OH^- absorbance at 25 and 300 °C.

given the small differences in the solution composition. This arises because the same species is absorbing and the concentration of this species is independent of pH in the acid to near neutral region. This species can be ascribed to unionised $H_3AsO_3^0$. Thus, if one also considers the ionisation of arsenous acid (i.e., reaction (12)), then in addition to OH^-, the other two absorbing species would be $H_3AsO_3^0$ and $H_2AsO_3^-$. The molar absorptivity of H_3AsO_3 at any given temperature was obtained from absorbance measurements in acid solutions (i.e., in the absence of any other absorbing species). Fig. 10 shows the spectra, corrected for hydroxide ion absorbance at 25 and 300 °C. The absorbances are due only to the presence of arsenic(III) species. Fig. 11 gives the molar absorptivities of $H_3AsO_3^0$ and $H_2AsO_3^-$ at different temperatures. The molar absorptivity of $H_2AsO_3^-$, resulting from the substraction of contribution from both OH^- and H_3AsO_3, shows a strong red shift in the band position with increasing temperature (Fig. 11). The shift of the $H_2AsO_3^-$ absorption band is typical of a charge-transfer-to-solvent (ctts) transitions noted for other anionic species (e.g., OH^-, HS^-, Cl^-, and ClO_4^-). The linear dependence of the absorption maximum with temperature (Fig. 12) is a

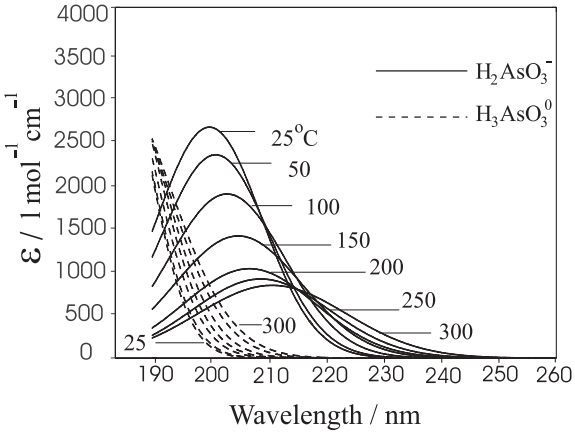

Fig. 11. Molar absorptivities, ε, of $H_3AsO_3^0$ and $H_2AsO_3^-$ from 25 to 300 °C at the saturated vapour pressure.

further indication of a charge-transfer-to-solvent transition. The absorption maximum at 25 °C for the undissociated arsenous acid species is at the edge of the vacuum UV region at approximately 186 nm. For the deprotonated arsenous acid species, the band maximum is shifted to 202 nm. Fig. 13 shows the deconvoluted spectrum at 25 °C and for a solution having a total arsenic(III)

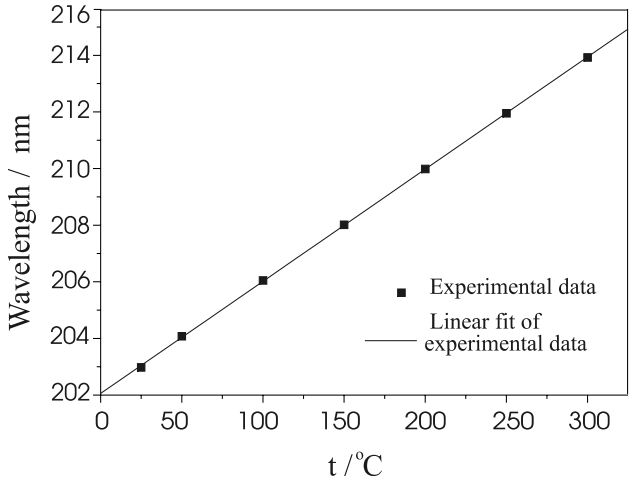

Fig. 12. Temperature dependence of the absorption maximum of the $H_2AsO_3^-$ species.

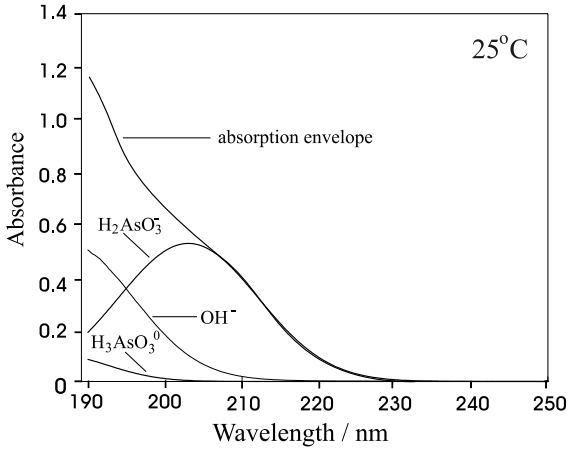

Fig. 13. The deconvoluted spectrum for a solution having As(III) = 9.39×10^{-5} mol/dm^3 and $OH^- = 1.32 \times 10^{-4}$ mol/dm^3.

concentration of 9.39×10^{-5} mol/dm^3 and $OH^- = 1.32 \times 10^{-4}$ mol/dm^3 (i.e., spectrum (e) in Fig. 2).

The values of the equilibrium constants obtained in the non-linear least squares refinement are summarised in Table 5 and presented together with the few existing literature data in Fig. 14. The higher uncertainties associated with the values of $pK_1 \geqslant 200$ °C arise from the coincidence of the charge-transfer-to-solvent band for

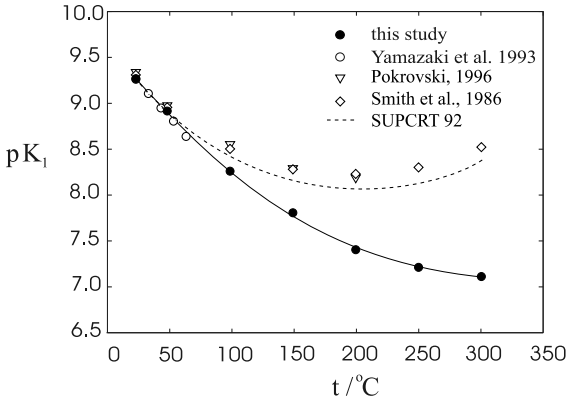

Fig. 14. Temperature dependence of the ionisation constant (molal) of arsenous acid up to 300 °C and at saturated vapour pressures.

the hydroxide ion red shifting at a faster rate than the arsenous acid species bands such that extensive band overlap occurs with resulting higher absorbances. Data from this study are in good agreement with other data at 25 °C (Table 1) and with the data from Yamazaki et al. (1993) up to 65 °C as well as with the data extrapolated to a zero ionic strength from Antikainen and Tevanen (1961) up to 45 °C. In addition, the equilibrium stability constant for the deprotonation of arsenous acid from SUPCRT92 (Johnson et al., 1992) as well as the estimated values given by Smith et al. (1986) are also shown in Fig. 14 for comparison. However, these values differ from our experimentally determined values by up to 1.5 orders of magnitude at 300 °C. The values for pK_1 reported by Pokrovski (1996) are similarly discrepant at higher temperatures.

In order to derive the thermodynamic functions for the ionisation constants from our experimental data, the values of $\log K_1$ as a function of temperature were fitted to different forms of

$$\log_{10} K_1 = A + BT + CT^2 + D/T + E\log T, \quad (15)$$

where T is in Kelvin. A three term expression (see Table 6) was found to best fit the data and was subsequently differentiated to provide values of the standard enthalpy and entropy change of arsenous acid ionisation.

Table 5
The ionisation constant (molal) of arsenous acid from 25 to 300 °C at the saturated vapour pressure, where the uncertainty is 2σ

T (°C)	pK_1
25	9.25 ± 0.05
50	8.90 ± 0.05
100	8.25 ± 0.05
150	7.80 ± 0.09
200	7.40 ± 0.17
250	7.21 ± 0.23
300	7.11 ± 0.14

Table 6
Thermodynamic data calculated from our experimental data for arsenous acid ionisation reaction (12) at the saturated vapour pressure using the expression, $\log_{10} K_1 = -16.1636 + 0.0312T - 0.0000268T^2$

T (°C)	ΔG° (kJ mol^{-1})	ΔH° (kJ mol^{-1})	ΔS° (J mol^{-1}K^{-1})
25	52.77	21.62	−104.5
50	55.03	25.26	−92.1
100	58.91	33.31	−68.6
150	63.16	42.36	−49.2
200	67.00	52.35	−30.9
250	72.17	63.27	−17.0
300	77.98	75.06	−5.1

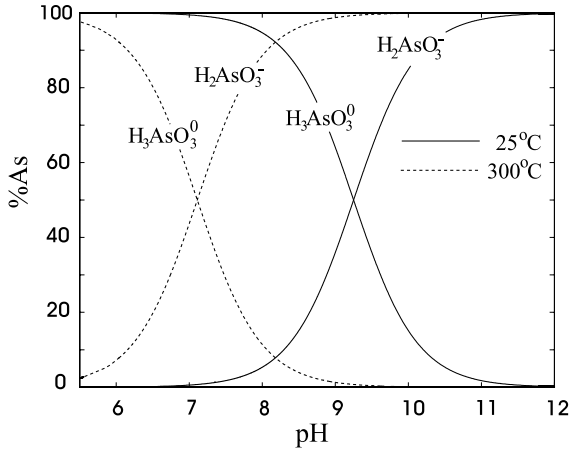

Fig. 15. The distribution of arsenous acid species as a function of pH at 25 and 300 °C at the saturated vapour pressure.

4. Conclusions

Over the temperature range from 25 to 300 °C, the ionisation constant, pK_1, decreases by more then two orders of magnitude from 9.25 to 7.11. In low sulphur containing hydrothermal fluids in the Earth's crust, the arsenic chemistry will also be dominated by the two arsenous acid species, H_3AsO_3 and $H_2AsO_3^-$. In rock-buffered, epithermal ore fluids, as much as 30% of the total dissolved arsenic could be transported as the $H_2AsO_3^-$ species (see Fig. 15). The extent of ion pairing of $H_2AsO_3^-$ with various cations present in natural multicomponent, electrolyte solutions in the Earth's crust is unknown. The formation and stability of thioarsenite species in aqueous media will be the subject of a further communication. At higher temperatures, boiling/phase separation leads to an increase in pH and volatile loss (i.e., CO_2, H_2S, etc) in natural hydrothermal systems. This causes the formation of $H_2AsO_3^-$ (Fig. 15) which will in turn have an effect on the hydrothermal, arsenic-containing mineral equilibria. Finally, we note that the electrospray mass spectrometric data suggest that the AsO_2^- stoichiometry apparently predominates in low density aqueous media.

Acknowledgments

This project was supported by ETH research funding awarded to T.M. Seward. We thank Dr. R. Kissner (Dept. Chemie, ETH) for help with the mass spectrometric measurements. We also thank two anonymous reviewers and Dr. L.G. Benning for their helpful reviews of our manuscript.

Associate editor: Liane G. Benning

References

Antikainen, P.J., Tevanen, K., 1961. The effect of temperature on the ionization of arsenious acid. *Suom. Kemistil.* **34**, 3–4.

Antikainen, P.J., Rossi, V.M.K., 1959. Chelation of arsenious acid with polyols. *Suom. Kemistil.* **32B**, 185–189.

Britton, H.T.S., Jackson, P., 1934. Physicochemical studies of complex formation involving weak acids. Part X. Complex formation between tartaric acid and (a) arsenic acid, (b) arsenous acid, (c) antimonous hydroxide, in acid and alkaline solutions. The dissociation constants of arsenous and arsenic acids. *J. Chem. Soc.*, 1048–1055.

Caldwell, B.K., Caldwell, J.C., Mitra, S.N., Smith, W., 2003. Searching for an optimum solution to the Bangladesh arsenic crisis. *Soc. Sci. Med.* **56**, 2089–2096.

Chaillou, G., SchSfer, J., Anschutz, P., Lavaux, G., Blanc, G., 2003. The behaviour of arsenic in muddy sediments of the Bay of Biscay (France). *Geochim. Cosmochim. Acta* **67**, 2993–3003.

Criaud, A., Fouillac, C., 1989. The distribution of arsenic(III) an arsenic(V) in geothermal waters: examples from the Massif Central of France, the Island of Dominica in the Leeward Islands of the Caribbean, the Valles Caldera of New Mexico, USA, and southwest Bulgaria. *Chem. Geol.* **76**, 259–269.

Debusschere, L., Demesmay, C., Rocca, J.L., 2000. Arsenic speciation by coupling capillary zone electrophoresis with mass spectrometry. *Chromatographia* **51**, 262–268.

Ellis, A.J., Mahon, W.A.J., 1977. *Chemistry and Geothermal Systems*. Academic Press, New York.

Frisch, M.J., Trucks, G.W., Schlegel, H.B., Cheeseman, J.R., Zakrzewski, V.G., Montgomery, Jr. J.A., Stratmann, R.E., Burant, J.C., Dapprich, S., Millam, J.M., Daniels, A.D., Kudin, K.N., Strain, M.C., Farkas, O., Tomasi, J., Barone, V., Cossi, M., Cammi, R., Mennucci, B., Pomelli, C., Adamo, C., Clifford, S., Ochterski, J., Petersson, G.A., Ayala, P.Y., Cui, Q., Morokuma, K., Salvador, P., Dannenberg, J.J., Malick, D.K., Rabuck, A.D., Raghavachari, K., Foresman, J.B., Cioslowski, J., Ortiz, J.V., Baboul, A.G., Stefanov, B.B., Liu, G., Liashenko, A., Piskorz, P., Komaromi, I., Gomperts, R., Martin, R.L., Fox, D.J., Keith, T., Al-Laham, M.A., Peng, C.Y., Nanayakkara, A., Challacombe, M., Gill, P.M.W., Johnson, B., Chen, W., Wong, M.W., Andres, J.L., Gonzalez, C., Head-Gordon, M., Replogle, E.S., Scuseria, G.E., Robb, M.A., Pople, J.A., 2001. Gaussian, 98 (Revision A.11). Gaussian, Inc. 2001. Pittsburgh PA.

Garrett, A.B., Holmes, O., Laube, A., 1940. The solubility of arsenous oxide in dilute solutions of hydrochloric acid and sodium hydroxide. The character of the ions of trivalent arsenic. Evidence for polymerization of arsenous acid. *J. Am. Chem. Soc.* **62**, 2024–2028.

Gout, R., Pokrovski, G., Schott, J., Zwick, A., 1997. Raman spectroscopic study of arsenic speciation in aqueous solutions up to 275 °C. *J. Raman Spectrosc.* **28**, 725–730.

Haar, L., Gallagher, J.S., Kell, G.S., 1984. *NBS/NRC Steam tables. Thermodynamic and Transport Properties and Computer Programs for Vapour and Liquid States of Water in SI Units*. Hemisphere Publ. Corp.

Heinrich, C.A., Eadington, P.J., 1986. Thermodynamic predictions of the hydrothermal chemistry of arsenic, and their significance for the paragenetic sequence of some cassiterite–arsenopyrite-base metal sulfide deposits. *Econ. Geol.* **81**, 511–529.

Ho, P.C., Bianchi, H., Palmer, D.A., Wood, R.H., 2000. Conductivity of dilute aqueous electrolyte solutions at high temperatures and pressures using a flow cell. *J. Sol. Chem.* **29**, 217–235.

Ivakin, A.A., Vorobeva, S.V., Gertman, E.M., Voronova, E.M., 1976. Acid–base equilibria and self-association in arsenic acid solutions. *Zhurn. Neorgan. Khim.* **21**, 442–448.

Johnson, J.W., Oelkers, E.H., Helgeson, H.C., 1992. Supcrt92—a software package for calculating the standard molal thermodynamic properties of minerals, gases, aqueous species, and reactions from 1 to 5000 bar and 0 to 1000 °C. *Comp. Geosci.*, 18.

Krupp, R.E., Seward, T.M., 1987. The Rotokawa geothermal system, New-Zealand—an active epithermal gold-depositing environment. *Econ. Geol.* **82**, 1109–1129.

Loehr, T.M., Plane, R.A., 1968. Raman spectra and structures of arsenious acid and arsenites in aqueous solution. *Inorg. Chem.* **7**, 1708–1714.

Morozov, V.A., 1993. *Regulization Methods for Ill-posed Problems*. CRS Press, Bocka Raton, FL, 257 pp.

Newman, D.K., Beveridge, T.J., Morel, F.M.M., 1997. Precipitation of arsenic trisulfide by *Desulfotomaculum auripigmentum*. *Appl. Environ. Microbiol.* **63**, 2022–2028.

Nickson, R.T., McArthur, J.M., Ravenscroft, P., Burgess, W.G., Ahmed, K.M., 2000. Mechanism of arsenic release to groundwater, Bangladesh and West Bengal. *Appl. Geochem.* **15**, 403–413.

Nishida, S., Kimura, M., 1989. Kinetic-studies of the oxidation reaction of arsenic(III) to arsenic(V) by peroxodisulfate ion in aqueous alkaline media. *J. Chem. Soc., Dalton Trans.* **2**, 357–360.

Pliego, J.R., Riveros, J.M., 2002. Gibbs energy of solvation of organic ions in aqueous and dimethyl sulfoxide solutions. *Phys. Chem. Chem. Phys.* **4**, 1622–1627.

Pokrovski, G.S., 1996. Etude experimentale du comportement du germanium, du silicium et de l'arsenic et de la complexation de l'aluminium avec la silice dans les solutions naturelles. Ph.D. thesis, Universite Paul-Sabatier, Toulouse, France.

Pokrovski, G., Gout, R., Schott, J., Zotov, A., Harrichoury, J.C., 1996. Thermodynamic properties and stoichiometry of As(III) hydroxide complexes at hydrothermal conditions. *Geochim. Cosmochim. Acta* **60**, 737–749.

Pokrovski, G.S., Zakirov, I.V., Roux, J., Testemale, D., Hazemann, J.L., Bychkov, A.Y., Golikova, G.V., 2002. Experimental study of arsenic speciation in vapor phase to 500 °C: implications for As transport and fractionation in low-density crustal fluids and volcanic gases. *Geochim. Cosmochim. Acta* **66**, 3453–3480.

Polya, D.A., Lythgoe, P.R., Abou-Shakra, F., Gault, A.G., Brydie, J.R., Webster, J.G., Brown, K.L., Nimfopoulos, M.K., Michailidis, K.M., 2003. IC-ICP-MS and IC-ICP-HEX-MS determination of arsenic speciation in surface and groundwaters: preservation and analytical issues. *Min. Mag.* **67**, 247–261.

Raposo, J.C., Sanz, J., Zuloaga, O., Olazabal, M.A., Madariaga, J.M., 2003. Thermodynamic model of inorganic arsenic species in aqueous solutions. Potentiometric study of the hydrolytic equilibrium of arsenious acid. *J. Sol. Chem.* **32**, 253–264.

Reyes, A.G., Trompetter, W.J., Britten, K., Searle, J., 2003. Mineral deposits in the Rotokawa geothermal pipelines, New Zealand. *J. Volcanol. Geotherm. Res.* **119**, 215–239.

Robinson, R.A., Stokes, R.H., 1968. *Electrolyte Solutions*. Butterworths, London.

Romero, L., Alonso, H., Campano, P., Fanfani, L., Cidu, R., Dadea, C., Keegan, T., Thornton, I., Farago, M., 2003. Arsenic enrichment in waters and sediments of the Rio Loa (Second Region, Chile). *Appl. Geochem.* **18**, 1399–1416.

Ryu, J.I., Gao, S., Dahlgren, R.A., Zieren, R.A., 2002. Arsenic distribution, speciation and solubility in shallow groundwater of Owens Dry Lake, California. *Geochim. Cosmochim. Acta* **66**, 2981–2994.

Salmassi, T.M., Venkateswaren, K., Satomi, M., Nealson, K.H., Newman, D.K., Hering, J.G., 2002. Oxidation of arsenite by *Agrobacterium albertimagni*, AOL15, sp. nov., isolated from Hot Creek, California. *Geomicrobiology* **19**, 53–66.

Salomaa, P., Hakala, R., Vesala, S., Aalto, T., 1969. Solvent deuterium isotope effects on acid–base reactions 3. Relative acidity constants of inorganic oxyacids in light and heavy water. Kinetic applications. *Acta Chem. Scand.* **23**, 2116–2126.

Smedley, P.L., Kinniburgh, D.G., 2002. A review of the source, behaviour and distribution of arsenic in natural waters. *Appl. Geochem.* **17**, 517–568.

Smith, C.L., Ficklin, W.H., Thompson, J.M., 1987. Concentrations of arsenic, antimony, and boron in steam and steam condensate at the Geysers, California. *J. Volcanol. Geotherm. Res.* **32**, 329–341.

Smith, R.W., Popp, C.J., Norman, D.I., 1986. The dissociation of oxy-acids at elevated-temperatures. *Geochim. Cosmochim. Acta* **50**, 137–142.

Takano, Y., Houk, K.N., 2005. Benchmarking the conductor-like polarizable continuum model (CPCM) for aqueous solvation free energies of neutral and ionic organic molecules. *J. Chem. Theory Comp.* **1**, 70–77.

Tossell, J.A., 1997. Theoretical studies on arsenic oxide and hydroxide species in minerals and in aqueous solution. *Geochim. Cosmochim. Acta* **61**, 1613–1623.

Webster, J.G., Nordstrom, D.K., 2003. Geothermal arsenic. In: *Arsenic in Ground Water*. Kluwer Academic Publishers, Boston, pp. 101–125.

Weissberg, B.G., Browne, P.R.L., Seward, T.M., 1979. Ore metals in active geothermal systems. In: Barnes, H.L. (Ed.), *Geochemistry of Hydrothermal Ore Deposits*. John Wiley and Sons, Inc., pp. 738–780.

Yamazaki, H., Sperline, R.P., Freiser, H., 1993. Spectrophotometric determination of the dissociation constant (pK_a) of arsenious acid. *Anal. Chem. Acta* **284**, 379–384.

Yokoyama, T., Takahashi, Y., Tarutani, T., 1993. Simultaneous determination of arsenic and arsenious acids in geothermal water. *Chem. Geol.* **103**, 103–111.